Tissue Barriers 4:1, e1142493; January/February/March 2016; Published with license by Taylor & Francis Group, LLC

Microfluidic organ-on-chip technology for blood-brain barrier research

Marinke W van der Helm[1,*] Andries D van der Meer[2], Jan C T Eijkel[1], Albert van den Berg[1], and Loes I Segerink[1]

[1]BIOS Lab on a Chip group; MIRA Institute for Biomedical Technology and Technical Medicine & MESA+ Institute for Nanotechnology; University of Twente; Enschede, The Netherlands; [2]Applied Stem Cell Technologies; MIRA Institute for Biomedical Technology and Technical Medicine; University of Twente; Enschede, The Netherlands

Keywords: BBBs-on-chips, blood-brain barrier, endothelial cells, microfabrication, microfluidics, organs-on-chips

Abbreviations: AC, Alternating current; ACM, Astrocyte-conditioned medium; bEnd.3, Mouse brain endothelial cell line; BBB, Blood-brain barrier; DC, Direct current; EC, Endothelial cell; FITC, Fluorescein isothiocyanate; hBMVEC, Primary human brain-derived microvascular endothelial cell; hCMEC/D3, Human cerebral microvascular endothelial cell line; (h)iPSC, (Human) induced pluripotent stem cell; HUVEC, Human umbilical vein endothelial cell; NVU, Neurovascular unit; PC, Polycarbonate; PE, Polyester; PTFE, Polytetrafluoroethylene; PDMS, Poly(dimethyl siloxane); Pgp, P-glycoprotein; RBE4, Rat brain endothelial cell line; TEER, Transendothelial electrical resistance; TNF-α, Tumor necrosis factor α; ZO-1, Zonula occludens 1 (tight junction protein)

Organs-on-chips are a new class of microengineered laboratory models that combine several of the advantages of current *in vivo* and *in vitro* models. In this review, we summarize the advances that have been made in the development of organ-on-chip models of the blood-brain barrier (BBBs-on-chips) and the challenges that are still ahead. The BBB is formed by specialized e3ndothelial cells and separates blood from brain tissue. It protects the brain from harmful compounds from the blood and provides homeostasis for optimal neuronal function. Studying BBB function and dysfunction is important for drug development and biomedical research. Microfluidic BBBs-on-chips enable real-time study of (human) cells in an engineered physiological microenvironment, for example incorporating small geometries and fluid flow as well as sensors. Examples of BBBs-on-chips in literature already show the potential of more realistic microenvironments and the study of organ-level functions. A key challenge in the field of BBB-on-chip development is the current lack of standardized quantification of parameters such as barrier permeability and shear stress. This limits the potential for direct comparison of the performance of different BBB-on-chip models to each other and existing models. We give recommendations for further standardization in model characterization and conclude that the rapidly emerging field of BBB-on-chip models holds great promise for further studies in BBB biology and drug development.

*Correspondence to: Marinke W van der Helm;
Email: m.w.vanderhelm@utwente.nl
Submitted: 07/27/2015; Revised: 12/28/2015; Accepted: 01/02/2016
http://dx.doi.org/10.1080/21688370.2016.1142493

Introduction

Blood-brain barrier structure and function

The blood-brain barrier (BBB) comprises specialized endothelial cells and separates blood from brain interstitial fluids. Together with the choroid plexus which forms the blood-cerebrospinal fluid barrier, and the arachnoid epithelium, this barrier partitions blood and neural tissues in order to provide vital homeostasis in the brain.[1,2] The BBB serves as a physical and functional barrier which regulates passive and active transport, as well as a metabolic and immunological barrier.[1,2] The physical barrier is formed by the endothelial cells that are linked by tight junction proteins such as zonula occludens 1 (ZO-1) and claudin. These proteins form complexes that limit permeation of ions and hydrophilic agents via paracellular pathways.[1] The active transport barrier results from the expression of specific membrane transporters and vesicular mechanisms for exchange of specific essential nutrients and waste, and multidrug resistance transporters such as P-glycoprotein (Pgp) that regulate efflux of potentially harmful agents, including lipophilic agents.[1,2] The metabolic barrier is formed by enzymes that metabolize toxic compounds both intracellularly and extracellularly.[1] As a result of the physical and metabolic barrier, 98% of small-molecule and 100% of large-molecule drugs cannot cross the BBB.[3] Finally, the immunological barrier results from specialized regulation of the recruitment and transport of leukocytes and innate immune elements by the endothelium.[2]

The BBB is part of a larger structure: the neurovascular unit (NVU), consisting of endothelial cells forming the capillary, pericytes, glial cells and neuronal cells, as well as their associated extracellular matrix proteins.[1] The NVU anatomy is shown in **Figure 1**. The brain capillaries are comprised of tightly linked endothelial cells surrounded by pericytes and a basement membrane (30 to 40 nm thick lamina of a.o. collagen IV, laminin and fibronectin).[2] The microvessel is also surrounded by astrocytic end-feet and in close contact with microglia and neurons. All these

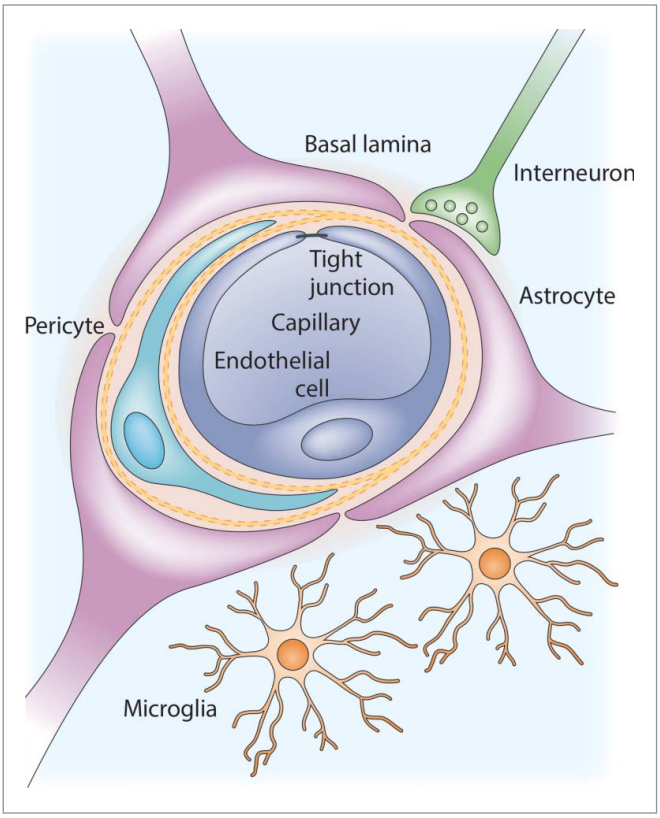

Figure 1. Anatomy of the neurovascular unit. A brain capillary comprised of specialized brain endothelial cells forms the blood-brain barrier (BBB). This capillary is surrounded by basal lamina (basement membrane), pericytes and astrocytic end-feet. Also microglia and neurons are in close contact with the BBB. Adapted by permission from Macmillan Publishers Ltd: Nature Reviews Neuroscience, ref. 4, copyright 2006.

elements have important roles in the formation, maturation and maintenance of the BBB.[2,4]

Current in vitro and in vivo models

In vivo techniques have provided the most reliable information in BBB research and are still regarded as the gold standard.[5] In pharmaceutical industry drug candidates are normally tested in animals before they are tested in humans. In these models the effects of drugs or treatments at the cellular, tissue, organ and systemic level can be monitored. Moreover, animal models allow the study of pharmacodynamics and pharmacokinetics, as well as of immunological responses. A general advantage of animal models is that they can represent the complexity of the BBB environment[6] and individual diversity found in humans. However, *in vivo* animal studies are costly, labor-intensive and ethically contentious.[7] In addition, the translation of animal models to the human clinic is difficult, evidenced by the statement that more than 80% of candidate drugs that were successfully tested in animal models failed in clinical trials.[8,9] This is partly caused by poor methodology and regulation of (some) animal experiments,[10-13] but also by inadequate reproduction of human pathophysiology by (genetically modified) animals[10-12] and by species-to-species variations in expression profiles of e.g. transporter proteins.[14]

As an alternative to animal testing, *in vitro* cell and tissue models are widely adopted and have been improved over the last few decades.[15] Generally, these models consist of cells grown in a controlled environment, making them relatively robust, reproducible, easy to analyze and more fit for high-throughput screening than animal studies.[16] However, these models are often too simple to answer complex research questions. For example, simple Petri dish cultures of brain endothelial cells may be useful to assess cytotoxicity of a drug candidate, but they are not fit for the study of drug transport through the BBB. To enable drug transportation studies, advances in the culture setup have been made, for example resulting in cell culture on a filter membrane suspended in a well, the so called Transwell setup.[17] This Transwell culture system is now a widely used *in vitro* platform for compartmentalized culturing. It provides a platform for drug studies and allows co-culture of endothelial cells and other cells that are associated with the NVU.[18] In addition, cells from human sources can be used in these models, which will avoid problems in translation of the results to the clinic that arise with *in vivo* animal models. However, these simple cultures still often fail to replicate key features of the BBB, such as shear stress resulting from blood flow and the BBB microenvironment (the NVU), which makes their predictive value for human responses questionable.[16]

In summary, *in vivo* animal models are regarded as the gold standard and allow study of cellular, tissue, organ and systemic level functions as well as pharmacodynamics and pharmacokinetics in a complex organism. However, they are costly, laborious, ethically contentious and often lack predictive value. In contrast, current *in vitro* models are more robust, reproducible, easy to analyze and fit for high-throughput than animal models and allow study of human cells and tissues. However, they are often too simplistic to answer complex research questions.

Organs-on-chips

To combine the advantages of *in vivo* and current *in vitro* models of tissues and organs, a new class of *in vitro* models has recently been introduced: organs-on-chips.[19] These so called chips are microfluidic devices in which tissues can be cultured in an environment that is engineered in such a way that it better replicates the *in vivo* microenvironment of that tissue.[16,20] This more physiologically relevant microenvironment can be achieved by engineering geometrical, mechanical and biochemical factors from the *in vivo* environment into a microfluidic device.[16] Another advantage of these organ-on-chip platforms is that imaging systems and sensors with real-time readouts can also be integrated.[19] Like in conventional *in vitro* methods, human cells or tissues can be included in organs-on-chips. Furthermore, these devices can be used for personalized (or precision) medicine when cells from a specific donor or group of donors are used. Both healthy and diseased tissues can be mimicked and tested in the same controlled environment. Moreover, organs-on-chips promise to replicate organ-level functions and allow the study of (patho)physiology on a higher level than could be achieved by conventional *in vitro* models. The comparison of organs-on-chips

Table 1. Comparison of organs-on-chips to current *in vivo* and in vitro methods.

	In vivo	In vitro	Organs-on-chips
Human tissue	No	Yes	Yes
Personalized/precision medicine	No	Yes	Yes
Realistic microenvironment	Yes	No	Yes[21,22]
Control over microenvironment	No	Yes	Yes[21]
Organ-level function	Yes	Limited	Potentially[21,22,24]
Real-time readouts	No	Limited	Yes[35]
High-throughput, parallelized testing	No	Yes	Possibly[45,62]
Pharmacodynamics / -kinetics	Yes	No	Potentially[36]

with current *in vivo* and *in vitro* methods is summarized in **Table 1**.

The first organ-on-chip papers have provided proof-of-principle that better replication of the microenvironment results in more physiological behavior of the tissues inside the organ-on-chip device and thus in better predictive value. Examples are the breathing lung-on-a-chip,[21] the bacteria-inhabited gut-on-a-chip[22,23] and the atherosclerosis-on-a-chip,[24] which show replication of organ-level functions and physiological responses to stimuli that could not have been studied before. More examples of such organ-on-chip applications are emerging rapidly.

BBB-on-chip models

As shown in the previous paragraphs, the use of microfluidic *in vitro* BBB models can improve BBB modeling by having more realistic dimensions and geometries, and by exposing the endothelium to physiological fluid flow.[17] In addition, in "BBBs-on-chips" not only the expression of specific markers can be tested (e.g., adherens and tight junction proteins), which can provide information on an organ-level function, but one can immediately study functionality: the permeability of the cell barrier. Permeability is now already routinely measured in compartmentalized cultures (e.g., Transwell models), but BBBs-on-chips hold promise to measure more BBB functions directly by incorporating sensors and real-time readouts. An additional example of a BBB function, which cannot be studied in Transwell, is the complex and specialized mechanism of recruitment of leukocytes at the BBB, analogous to the extravasation of leukocytes in the lung-on-a-chip in case of bacterial infection.[21] In addition, the recently discovered glymphatic pathway, which clears solutes from the brain and probably plays a role in neurodegenerative diseases, can be studied for the first time using microfluidic devices in which physiologically relevant blood pressure, intracranial pressure and flows can be applied.[25,26] When BBBs-on-chips are used to study such a complex biological phenomenon, they will provide deeper understanding of the BBB physiology and answer research questions that could not be answered before.[27] BBBs-on-chips then provide an extra tool for the BBB researchers' toolbox, next to classic *in vitro* cultures and *in vivo* animal studies. Depending on the research question, the most appropriate model can be chosen.

Current BBBs-on-chips

To this date, only ten publications of BBBs or NVUs-on-chips exist, to the best of our knowledge. In this section a summary is provided of all these microfluidic models of the BBB, in order of year of publication. In **Figure 2**, representative images are shown and key features of these models are summarized in **Table 2**. Next to these papers, numerous conference contributions indicate that the field of BBBs-on-chips is quickly moving forward, see for example refs. 28-34.

Booth and Kim published about their μBBB in 2012, which is shown in **Figure 2I**,[35] and have also published a follow-up paper in 2014.[36] Their device consists of polydimethylsiloxane (PDMS) parts with two channels (2 mm (luminal) or 5 mm (abluminal) wide, 200 μm deep), that are separated by a porous polycarbonate (PC) membrane (10 μm thick, 0.4 μm pores). The PDMS parts are sandwiched between two glass slides with sputtered thinfilm silver chloride (AgCl) electrodes in a four-point sensing structure to measure transendothelial electrical resistance (TEER) at near-direct current (DC) conditions. A mouse endothelial cell line (b.End3) was cocultured with a murine astrocytic cell line (C8D1A) on the opposite side of the membrane, which was coated with fibronectin. Both channels were perfused at 2.6 μL/min, which corresponds to a shear on the endothelial cells of approximately 2 mPa (calculated using the method presented later in this paper), which is low compared to the physiologically found shear of 0.3-2 Pa in brain capillaries.[37,38] The small height-to-width ratio ensured a mostly uniform shear stress across the channel width. TEER measurements yielded values of 180-280 $\Omega \cdot cm^2$, indicating the presence of a functional barrier. Apart from measuring the TEER, also permeability measurements of fluorescein isothiocyanate (FITC)-dextrans (4, 20, 70 kDa) and propidium iodide were used to confirm barrier function. Immunofluorescence showed the presence of tight junction protein ZO-1. In addition, the physiological effects of exposure to histamine and high pH were recorded. The TEER was higher and permeability lower inside the μBBB compared to conventional Transwell models, and coculture with astrocytes resulted in even more improved barrier functionality. The transient barrier disruption caused by histamine was monitored continuously by measuring TEER.[35]

In the second publication the authors further tested this model.[36] For these tests, they co-cultured b.End3 cells with the glial cell line C6 (from rat glial tumor) in the two channels coated with collagen IV/fibronectin and polylysine, respectively. The luminal channel width was increased to 4 mm to achieve an even more uniform shear stress across the channel width under dynamic conditions, which was 1.5 Pa at 2 mL/min. Again, presence of tight junction protein ZO-1 was confirmed with immunofluorescence. Toxicity of seven brain-targeting drugs was assessed by measuring lactate dehydrogenase (LDH) levels and after that the permeability coefficients of subtoxic levels of these drugs were measured in devices with a functional barrier, indicated by a sufficiently high TEER of over 150 $\Omega \cdot cm^2$. The authors showed that the measured permeability coefficients in their model under dynamic conditions correlated well with *in vivo* brain/plasma

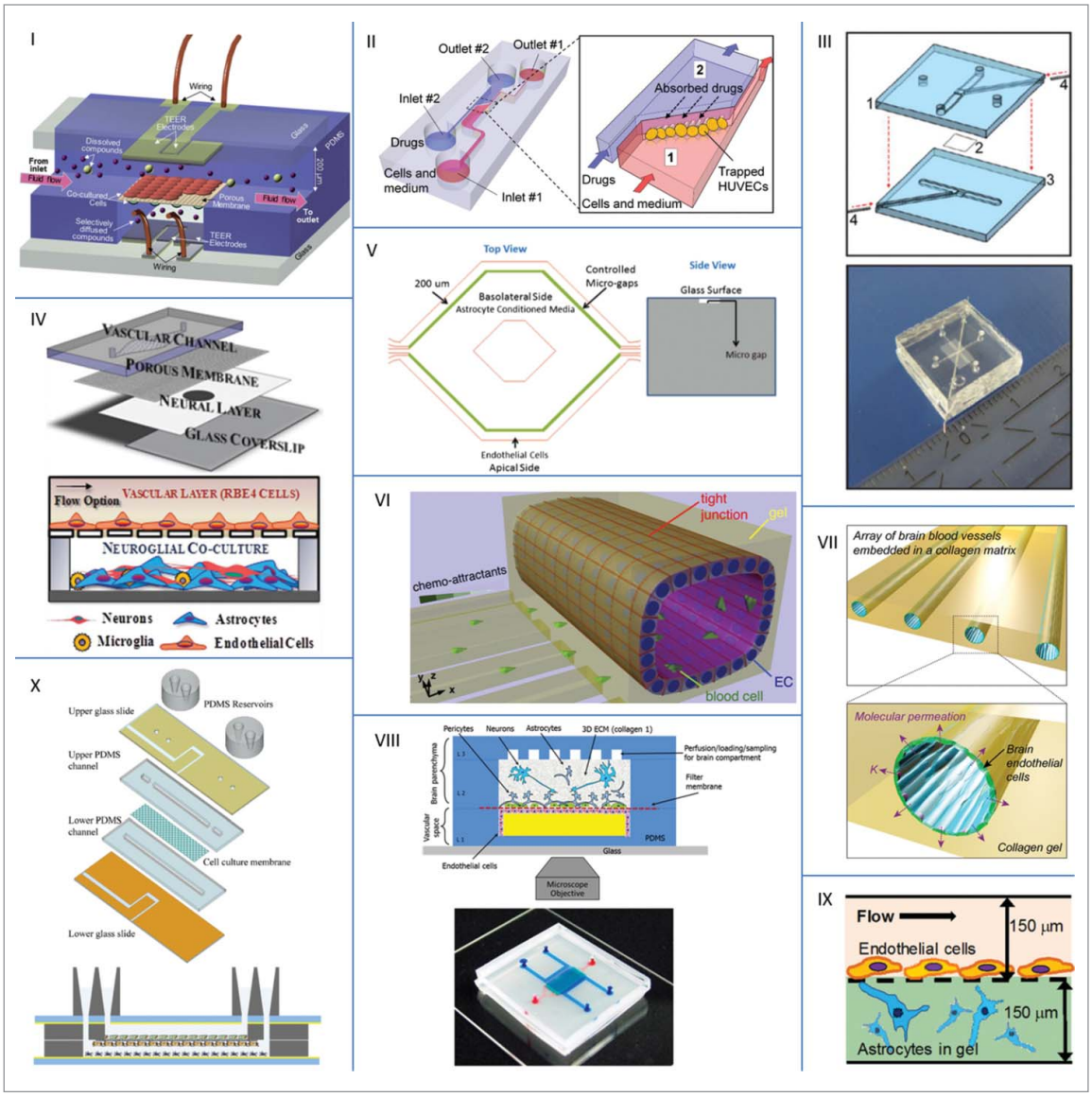

Figure 2. Examples of microfluidic BBB models from literature. Reprinted and adapted with permission from: **I** Booth[68]; **II** Yeon[69]; **III** Griep[70]; **IV** Achyuta[71]; **V** Prabhakarpandian[72]; **VI** Cho[44]; **VII** Kim[73]; **VIII** Brown[74]; **IX** Sellgren[75]; **X** Walter[76].

ratios, demonstrating the potential of this model for the prediction of clearance of drugs by the BBB.[36]

Also in 2012, Yeon *et al.* published about their permeability assay system for cerebral microvasculature, shown in **Figure 2II**.[39] This device, made of PDMS on glass, comprises two channels (25 μm high) connected by microholes (30 μm long, 5 μm high and 3 μm wide). By applying different flow rates in the two channels and thereby generating a pressure difference across the microholes, human umbilical cord endothelial cells (HUVECs) were trapped hydrodynamically in the microholes in close contact to each other. After 23 hours of incubation a barrier was formed. With immunofluorescence the presence of ZO-1 was shown. FITC-labeled dextrans (4, 40, 70 kDa) and various drugs were introduced at the other side of the microholes and the permeability of these agents through the HUVEC layer was assessed with fluorescence microscopy (real-time) and high-performance liquid chromatography (HPLC), respectively. The presence of astrocyte-conditioned medium (ACM) was found to decrease the permeability of the trapped HUVEC layer.[39]

Griep *et al.* published about their BBB-on-chip in 2013, which is shown in **Figure 2III**.[40] Their device consists of 2 PDMS parts with channel imprints (500 μm wide, 100 μm high), glued together with a PC membrane in between (10 μm thick, 0.4 μm pores). Cells from a human cerebral microvascular endothelial cell line (hCMEC/D3) were cultured in the top channel on top of the membrane, which was coated with collagen I. Barrier formation was monitored by determining TEER from impedance spectroscopy measurements with integrated platinum wire electrodes, positioned on either side of the membrane. After

two days a steady barrier was achieved and maintained up to 7 days with an average TEER (± standard error of the mean) of 37 $\Omega \cdot cm^2 \pm 0.9\ \Omega \cdot cm^2$, which is comparable to the value obtained in the conventional Transwell model (28 $\Omega \cdot cm^2 \pm 1.3\ \Omega \cdot cm^2$). The expression of tight junction protein ZO-1 was verified with immunofluorescence. In addition, the TEER of this BBB-on-chip increased up to 120 $\Omega \cdot cm^2$ when shear stress was applied (0.58 Pa at 2.5 mL/h flow) using a syringe pump. Upon addition of the inflammatory protein tumor necrosis factor α (TNFα) the TEER decreased to 12 $\Omega \cdot cm^2$.[40]

Achyuta *et al*. used a modular approach to create a NVU-on-a-chip, which was also published in 2013.[41] Their device, shown in **Figure 2IV**, consists of 2 parts that can be fabricated and used for cell culture separately and are assembled at a later stage. The neural part consists of a 8 mm diameter hole in a 100 μm thick PDMS layer on a cover slip. Freshly isolated E-18 rat cortical cells were cultured in this hole, which was coated with poly-D-lysine, for 10 days. The vascular part is a 10 mm wide, 100 μm high channel in PDMS with posts for support, glued on a PC membrane (7 μm thick, 8 μm pores). After coating with fibronectin, rat brain endothelial cells (RBE4 cell line) were cultured in this channel for 2 days under static conditions. After the specified culture periods, the device was assembled and functional tests were conducted. Live/dead staining showed good cell viability for both RBE4 and E-18 cells. Immunofluorescence showed proper differentiation of the neural culture and good endothelial function. The presence of tight junction protein ZO-1 was shown with Western blots. Barrier tightness was checked with A488dextran (3 kDa) leakage, perfused at 1 mL/h through the vascular channel and collected in the neuronal part. Less dextran was found in the neural reservoir in devices with a RBE4 cell layer compared to devices without cells, but more dextran leaked into the reservoir after the cells were exposed to TNFα.[41]

Also in 2013, Prabhakarpandian *et al*. published on their SyM-BBB which is shown in **Figure 2V**.[42] In a follow-up paper from 2015 Deosarkar and Prabhakarpandian *et al*. presented an adapted version of their model for neonatal BBB research, termed B^3C.[43] The SyM-BBB device, consisting of a PDMS part with channel structures on a glass slide, is designed to enable simultaneous imaging of the blood compartment (outer ring, 200 μm wide, 100 μm high) and the brain compartment (inner ring). The compartments are connected by micro-gaps (50 μm long, 3 μm wide, 3 μm deep) in the PDMS wall. RBE4 rat endothelial cells were cultured in the blood compartment, coated with fibronectin, to form a cell layer perpendicular to the gaps. During cell culture, fluidic shear was applied at 0.1 μL/min, corresponding to shear stress of approximately 3 mPa (calculated using the method presented in this paper), which is also low compared to the physiologically found shear of 0.3-2 Pa in capillaries.[37,38] ACM could be added to the brain compartment, which promoted tight junction formation. Barrier permeability was measured with FITC-labeled dextran (3-5 kDa) and the activity of the Pgp efflux transporter was assessed using rhodamine 123 with and without the transport inhibitor verapamil. In addition, the expression of Pgp and the tight junction proteins ZO-1 and claudin was checked using Western blots. In the presence of ACM the barrier permeability was decreased, the efflux activity was increased and the expression of tight junction proteins and Pgp was increased in these devices compared to devices without ACM and to conventional Transwells.[42]

In the B^3C chip adapted for neonatal BBB research presented in the follow-up paper from 2015 by Deosarkar *et al*.,[43] the shape of the channels was changed to circular, but the side-by-side orientation of the vascular channel and the brain compartment was retained. Primary neonatal rat brain capillary endothelial cells were cultured in the fibronectin-coated vascular channel under 0.01 μL/min flow using a syringe pump, resulting in a shear stress of 0.38 mPa. For co-culture conditions, primary rat astrocytes were seeded in the brain compartment, which was also coated with fibronectin. When astrocytes were present, the ZO-1 expression, as shown by immunofluorescence, was increased as well as the electrical resistance (which was not normalized to area to obtain the TEER), and the permeability for 40 kDa dextran-Texas red was decreased. Also astrocytic protrusions into the microgaps were seen, leading to cell-cell contact between endothelial cells and astrocytes. The permeability coefficient of 40 kDa dextran of the BBB inside the B^3C device was more comparable to the *in vivo* BBB permeability, measured through a cranial window in 2-weeks old anesthetized rats, than the BBB in Transwells. Furthermore, neonatal endothelial cells showed weaker ZO-1 expression than adult cells, but in the presence of ACM they showed a bigger decrease in permeability and increase in electrical resistance than adult endothelial cells.[43]

In 2015, Cho *et al*. published on their 3-dimensional BBB model, which is shown in **Figure 2VI**.[44] Their device consists of a PDMS part with channel imprints on a glass-bottomed well plate. An acrylic well plate with reservoirs for culture medium was glued to the top of the device. In the PDMS there are an endothelial channel and a brain channel (both 50 μm high) and an array of small perpendicular side channels (5 μm high) connecting the 2 main channels. After coating the channels with poly-D-lysine, the channels were filled with a collagen I gel which was replaced again by cell culturing medium in the endothelial chambers, resulting in a thin collagen gel on the walls. RBE4 rat endothelial cells were seeded in the device and allowed to attach to both the top and bottom surface. Medium was refreshed every day by adding 100 μL fresh medium to one reservoir and removing the same amount of old medium from the other reservoir. After obtaining a monolayer (2-3 days) the barrier function was tested by adding 40 kDa dextran-FITC to the endothelial chamber and following the increase in fluorescence in the side channels in time. It took significantly longer for the gradient to reach saturation in a device with RBE4 cells (7 minutes) than in a device without cells (4 minutes). The transmigration of neutrophils across the endothelial barrier and through the side channels was recorded. Upon addition of a chemoattractant (interleukin 8) to the brain channel more neutrophils transmigrated than when no chemoattractant was added. Next, neuroinflammation was mimicked by exposing the BBB to TNF-α. From the cytokine release profile it was concluded that the treatment had elicited an inflammatory effect on the BBB model. In addition, the ZO-1

expression was also shown to decrease. Lastly, they used their platform to study ischemia by exposing the endothelium to low oxygen and low glucose (anaerobic gas and DMEM without glucose) and subsequently allowing reoxygenation under normal conditions. Formation of reactive oxygen species and activation of Rho kinase as a result of oxidative stress was confirmed, as well as a decrease in ZO-1 expression. Upon addition of antioxidants to counter the reactive oxygen species, the ZO-1 expression level slightly increased after 3 hours but decreased again after 6 hours.[44]

Also in 2015, Kim *et al*. reported a collagen-based 3D model of brain vasculature, shown in **Figure 2VII**.[45] Their device is comprised of tubes in a collagen I gel (235-360 μm diameter), resulting from pouring collagen I around microneedles in a 3D printed frame to which fluidic connectors can be coupled. After the microneedles were removed, the resulting tubes were coated with fibronectin. Endothelial cells from the bEnd.3 mouse cell line were cultured in these tubes to replicate the BBB. Immunofluorescence showed intact vessels after 14 days with ZO-1 expression. FITC-labeled dextran (40 kDa) was introduced to the tubes and under static conditions the transendothelial permeability was monitored with fluorescence images taken at certain time intervals, showing an intact cell layer after 7 days. Using a mathematical model they were able to derive permeability coefficients from these images. Upon exposure to mannitol, barrier disruption was seen in the permeability measurements as expected. Long-term recovery of the barrier function was also shown after mannitol was removed.[45]

Brown *et al*. published on the NVU chip in 2015, which is shown in **Figure 2VIII**.[46] Their chip consists of three PDMS layers: a vascular chamber with inlet channels (100 μm high and 6.2 mm wide), a brain chamber (4.75 mm wide and 6.2 mm long, 500 μm deep) and a layer with brain perfusion channels (several parallel channels, 100 μm high). The vascular and brain chambers are separated by a PC membrane (0.2 μm pores). Prior to cell seeding the NVU devices were coated with laminin. Primary human brain-derived microvascular endothelial cells (hBMVEC) were cultured on the membrane in the vascular chamber, which was held upside down and under a constant flow of 2 μL/min. This corresponds to a shear stress of 2 mPa (calculated using the method presented later in this paper), which is also low compared to the physiologically found shear of 0.3-2 Pa in capillaries.[37,38] After 12 days the device was flipped right-side up and pericytes and astrocytes were loaded in the brain chamber. After two days of culture under flow, the brain chamber was filled with a collagen I matrix with suspended human induced pluripotent stem cell (hiPSC)-derived neurons. The gel was allowed to set for 2 hours and subsequently the device was perfused for 3 days before testing the BBB. The cells remained viable up to 21 days, as was shown with live/dead staining (>80 % cell viability). Using immunofluorescence staining the presence of tight junctions (ZO-1) was shown and also the percentage of actin filaments that were aligned with the flow direction was quantified. The cells significantly blocked diffusion of FITC-dextrans (10 and 70 kDa) from the vascular chamber to the brain perfusion channels, but the permeability was shown to increase in the presence of glutamate, which is known to disrupt tight junctions. In addition, the active transport of ascorbate and its function of reducing permeability was demonstrated. Using a 4-point impedance sensing method the TEER was measured. Measurements showed an increase in TEER during the 12-day culture period of the endothelial cells. The authors reported resistance values of 30000-33000 Ω/cm^2 for devices with endothelial cells and 7500 Ω/cm^2 for empty devices, which corresponds to a TEER of 1950-2210 $\Omega \cdot cm^2$ for a membrane area of $4.75 \cdot 6.2$ mm^2 when the resistance of the empty is subtracted. Exposing the devices to 33°C ("cold shock") resulted in a significant decrease in TEER.[46]

Sellgren *et al*. published in 2015 on the microfluidic NVU model of which an image is shown in **Figure 2IX**.[47] Their chip comprises 2 PDMS parts with channel imprints with a polytetrafluoroethylene (PTFE) or polyester (PE) membrane in between (0.4 μm pores and 40 or 10 μm thick, respectively). The vascular channel was 10 mm long, 1 mm wide and 150 μm high, while the basolateral compartment was 150-300 μm high. Astrocytes from the murine C8D1A cell line were suspended in a collagen hydrogel and loaded in the basolateral compartment. After coating with collagen IV-fibronectin (PE) or collagen I (PTFE), cells from the bEnd.3 cell line were cultured on the membrane in the vascular channel under a fluid flow of 120 μL/min, resulting in a physiologically relevant shear stress of 0.5 Pa. Both membranes were transparent and allowed monitoring of monolayer formation with phase contrast microscopy. After a monolayer was obtained, the collagen gel containing the astrocytes was flushed out and the endothelial barrier function was tested by adding 70 kDa FITC-dextran to the vascular channel and collecting medium from the basolateral channel every 30 minutes. The apparent permeability coefficient of a device with bEnd.3 cells was significantly lower than for a device without cells. The PTFE membrane was able to support monolayer survival under physiological shear stress and immunofluorescence showed claudin-5 expression, while the cells did not show claudin-5 on the PE membrane and were peeled off at the same flow rate. Therefore, it was concluded that PTFE membranes are more suitable to support cell attachment and relevant shear stress than PE.[47]

In 2016, Walter *et al*. published about their barrier-on-a-chip device, which is shown in **Figure 2 X**.[48] Their device was used to recreate the BBB, of which the results are summarized here, as well as intestinal and lung epithelial barriers. Their device consists of 2 PDMS parts with channels (both 200 μm wide and 200 μm high), that are separated by a porous PET membrane (23 μm thick, 0.45 μm pores), fixated with a silicone sealant. The PDMS parts are sandwiched between 2 glass slides with sputter-coated 25 nm thick transparent gold electrodes and fixated with a silicon sealant. The electrodes are positioned in a 4-point sensing structure to measure TEER at near-DC conditions. Two PDMS blocks with reservoirs are plasma-bonded to the top glass slide. Prior to use the blood channel was coated with collagen I and the brain compartment with collagen IV. Two different cell models were used: hCMEC/D3 cells and primary rat endothelial cells co-cultured with primary astrocytes and pericytes. The endothelial cells were cultured on top of the membrane in the top channel. If present, the pericytes were cultured on the

bottom of the membrane and the astrocytes on the bottom of the bottom channel. The cells were maintained under static conditions for 3 days, after which a peristaltic pump provided dynamic culture conditions at low shear stress (rapported to be 0.15 dyn, but 0.15 dyn/cm^2 = 15 mPa was meant). Barrier properties were induced with lithium chloride and tightened with a cyclic adenosine monophosphate derivate (CPT-cAMP) and a phosphodiesterase inhibitor (RO). The TEER of hCMEC/D3 barriers was (mean ± standard deviation) 19 ± 2.8 Ω·cm^2 under static conditions and increased to 29 ± 7.2 Ω·cm^2 under dynamic conditions. The latter value is higher than the TEER measured in Transwell system (28 ± 3.5 Ω·cm^2). The apparent permeability was measured statically by determining the concentration in the brain compartment at different time intervals. The apparent permeability coefficient for FITC-dextran (4.4 kDa) and Evans blue-albumin (67 kDa) was lower for dynamic conditions than for static conditions, but the permeability for sodium fluorescein (376 Da) did not change significantly. Confocal microscopy confirmed the presence of tight junction protein ZO-1 and adherens junction protein β-catenin. The TEER of the primary rat BBB in the device was 114 ± 38 Ω·cm^2 for both static and dynamic culture conditions, which was lower than the TEER on culture inserts (173 ± 22 Ω·cm^2). The apparent permeability coefficient for fluorescein was lower under static conditions than under dynamic conditons. The permeability for the other two tracers did not differ significantly between these conditions. These cells expressed ZO-1 and β-catenin more strongly than hCMEC/D3 cells.[48]

Standardization challenges

As evidenced by the body of literature summarized in the previous section, significant steps have been taken toward developing physiological BBBs-on-chips. These recently reported chips show promising improvements when compared to conventional Transwell models: the exposure to fluid flow resulted in better barrier function.[35,36,40,42,48,49] and dynamic drug permeability studies in chips were found to be more predictive than in conventional static models.[36,43]

However, there are still challenges ahead for developing BBB-on-chip models that will become widely available for BBB-related research applications. One of them is to arrive at commonly accepted standards for quantitative evaluation of the functionality of a BBB-on-chip model.[6] In **Table 2** one can clearly see that both the device designs and the readout protocols vary greatly, as well as the used cell types. This shows the versatility of BBBs-on-chips and more generally of organ-on-chip technology, but this also complicates comparison between models. Therefore, in the following sections an overview is provided of aspects that need to be taken into consideration when designing and testing BBBs-on-chips and aspects that require consensus among researchers.

Permeability

As was mentioned in the introduction, the key function of the BBB is to provide homeostasis in the brain, and more specifically to protect the brain from harmful substances in the blood.[1] The performance of BBBs-on-chips should therefore be evaluated by measuring the permeability of the cell barrier. If this permeability is in agreement with physiological levels, then a valuable BBB-on-chip has been obtained which can be used for testing drug candidates. In general, large and hydrophilic molecules, for example dextrans and ions, are physically blocked by the tight junctions between endothelial cells. Ions and essential nutrients such as glucose, amino acids, peptides and hormones are transported actively into the brain by carriers and receptor mediated transport.[5] Small lipophilic molecules (MW < 400-500 Da) can cross the BBB without significant obstruction.[3] However, multi-drug resistance transporters regulate efflux of potentially harmful agents, including lipophilic agents.[1,2] To assess the full barrier function, analytes from all these classes have to be tested in the device: both hydrophilic and lipophilic molecules that are both passively and actively transported or excreted.

The determination of barrier permeability is demonstrated in almost all of the currently existing BBB devices (see **Table 2**).[35,36,39,41-48] However, it is important to quantify this permeability in such a way that it can be compared to *in vivo* and other *in vitro* data. For passive transport, this can be done by calculating the permeability coefficient of an analyte (cm/s), which is independent of the used analyte concentration, flow rate and device size, and can also be determined *in vivo*.[43,50] When an analyte is added to the luminal channel under constant flow and transport takes place toward the basal channel through the cell barrier on a membrane, the permeability coefficient can be determined with the following formulas:

$$P_{meas} = \frac{\dot{m}_a}{A \cdot (C_l - C_b)} = \frac{C_b \cdot Q}{A \cdot (C_l - C_b)} [cm/s].$$

In these formulas P_{meas} is the measured (or apparent) permeability coefficient (cm/s), $\dot{m}_a$ is the mass transport rate (mol/s) across the membrane which – when analyzing the sample flowing out of the basal compartment – can be quantified by multiplying the basal concentration C_b (mol/mL) with the applied flow rate in the basal channel Q (mL/s), A is the membrane area through which the transport takes place (cm^2) and C_l is the luminal concentration (mol/mL).[43,51] The permeability coefficient of the endothelial barrier, P_{endo}, can be calculated from this measured permeability coefficient P_{meas} and the permeability coefficient measured in a device without endothelium P_0 (blank) as follows:[35,36,43,51]

$$\frac{1}{P_{endo}} = \frac{1}{P_{meas}} - \frac{1}{P_0} [s/cm]$$

This endothelial permeability coefficient can then be compared to permeability coefficients found with the same analyte in other platforms. If there are more complex channel geometries the transport of analytes can also be modeled mathematically to arrive at a permeability coefficient, as was shown by Kim.[45] An advantage of measuring the permeability in microfluidic devices

Table 2. Summary of key features of the current BBBs-on-chips. "*N.A.*" indicates that the specified feature has not been measured or reported.

	Device materials (from bottom to top)	Size of blood compartment (width x height)	Membrane, thickness	Biological coating agents	Endothelial cells, co-cultured cells	Tight junction protein expression	Barrier permeability tracers	TEER	Physiological test	Shear stress (during culture)[a]
Booth Ref. 35, 36	Glass with electrodes – PDMS – PC – PDMS – glass with electrodes	2 mm x 200 μm	PC, 10 μm	Fibronectin Collagen IV + fibronectin (blood), polylysine (brain)	bEnd.3 (mouse EC), C8D1A (mouse astrocytes) bEnd.3 (mouse EC), C6 (rat)	ZO-1	FITC-dextrans (4,20,70 kDa), propidium iodide Various brain-targeting drugs	180-280 Ω·cm^2	Exposure to histamine, pH > 10 *N.A.*	0.08 mPa 1.5 Pa
Yeon Ref. 39	Glass - PDMS	25 μm high	Holes in PDMS wall, 30 μm long	*N.A.*	HUVEC (human), ACM	ZO-1	FITC-dextran (4,40,70 kDa) and various drugs	*N.A.*	*N.A.*	*N.A.*
Griep Ref. 40	PDMS – PC – PDMS	500 × 100 μm	PC, 10 μm	Collagen I	hCMEC/D3 (human)	ZO-1	*N.A.*	37-120 Ω·cm^2	Exposure to TNF-α	0.6 Pa
Achyuta Ref. 41	Glass – PDMS – PC – PDMS	10 mm x 100 μm	PC, 7 μm	Fibronectin (blood), poly-D-lysine (brain)	RBE4 (rat EC), E18 neural cells (rat)	ZO-1	A488-dextran (3 kDa)	*N.A.*	Exposure to TNF-α	*N.A.*
Prabhakar-pandian Ref. 42	Glass – PDMS	200 × 100 μm	3 μm holes in PDMS wall, 50 μm	Fibronectin	RBE4 (rat EC), ACM	ZO-1, claudin	FITC-dextran (3-5 kDa)	*N.A.*	Pgp function with rhodamine 123 / verapamil	3 mPa
Deosarkar Ref. 43					Primary rat EC, ACM, primary rat astrocytes	ZO-1	Texas red-dextran (40 kDa)	Only electrical resistance reported	*N.A.*	0.38 mPa
Cho Ref. 44	Glass – PDMS – acryl reservoirs	50 μm high	Side channels, 5 μm high	Poly-D-lysine + collagen I gel	RBE4 (rat EC)	ZO-1	FITC-dextran (40 kDa)	*N.A.*	Transmigration of neutrophils, TNF-α, ischemia	*N.A.*
Kim Ref. 45	Collagen in 3D printed frame	235-360 μm diameter	No membrane	Collagen I gel + fibronectin	bEnd.3 (mouse EC)	ZO-1	FITC-dextran (40 kDa)	*N.A.*	Exposure to mannitol	*N.A.*
Brown Ref. 46	PDMS – PC – PDMS – PDMS	6.2 mm x 100 μm	PC, thickness not specified	Laminin	hBMVEC, astrocytes, pericytes; hiPSC-derived neurons	ZO-1	FITC-dextran (10, 70 kDa)	1950-2210 Ω·cm^2 [b]	Glutamate exposure, active transport & barrier tightening with ascorbate, cold shock	2 mPa
Sellgren Ref. 47	PDMS – PTFE or PE – PDMS	1 mm x 150 μm	PTFE and PE, 40 μm and 10 μm respectively	Collagen I (PTFE), collagen IV + fibronectin (PE)	bEnd.3 (mouse EC), C8D1A (mouse astrocytes)	claudin-5	FITC-dextran (70 kDa)	*N.A.*	*N.A.*	0.5 Pa
Walter Ref. 48	Glass with electrodes – PDMS – PET – PDMS – glass with electrodes – PDMS reservoirs	200 μm x 200 μm	PET, 23 μm	Collagen I (blood), collagen IV (brain)	hCMEC/D3 or primary rat EC, astrocytes and pericytes	ZO-1	Fluorescein, FITC-dextran (4.4 kDa), Evans blue-albumin (67 kDa)	19-29 Ω·cm^2 (hCMEC/D3) 114 Ω·cm^2 (rat EC)	*N.A.*	15 mPa [c]

[a]Physiological shear stress lies between 0.3 and 2 Pa (3-20 dyn/cm^2).[37, 38] |

[b]These values were derived from the resistance values in Ω/cm^2 reported in the publication, corrected by the resistance of an empty device and the square of the measured area. |

[c]Shear stress was reported in dyn, but dyn/cm^2 was meant.

over Transwell systems is that the analyte can be supplied to the apical channel at a constant flow rate and the transported analyte can also be collected from the basal channel with a constant flow rate. In this way, the assumption that the concentration difference across the membrane stays constant throughout the measurement is met, while in static Transwell systems this difference decreases over time. In addition, a promising feature of organs-on-chips over static Transwell systems is the possibility for real-time monitoring of the permeability when on-line detection systems or fluorescence microscopy are used.[42,43]

A problem that can arise when performing permeability measurements in organs-on-chips is the contribution of other modes of transport than only diffusion (or active transport). For example, if there is a pressure difference between the two compartments, convective flow will result through gaps in the cell barrier. In addition, osmotic-driven flow can result if there is a difference in solute concentration between the channels. One has to be aware of these phenomena and limit their contribution in permeability measurements as much as possible, for example by having identical compartments with the same applied pressure and by using the same fluid (culture medium) on both sides of the barrier. Another factor that can influence permeability measurement is the presence of e.g., astrocytes at the basal side of the membrane. These are reported to have a tightening effect on the BBB, but they will also form a physical barrier against diffusion by themselves. So one should always check for the contribution of the presence of extra cells to the total barrier function.

Summarizing, the permeability of the cell layer is a very important readout of BBBs-on-chips. To validate physiological relevance, different analytes that are either passively or actively transported, excreted or metabolized should be tested with a suitable protocol. To enable comparison between platforms, a universal measure that is independent of the microdevice design, such as permeability coefficient, should be reported.

Transendothelial electrical resistance

Next to permeability, transendothelial electrical resistance (TEER) is a widely used quantity to assess barrier tightness.[1,52-55] TEER mostly represents the electrical resistance against paracellular transport: the tighter the cell layer is packed, the less gaps there will be in the cell barrier through which ions and other charged species can move, resulting in a higher resistance.[54] Only when the cell barrier is tight enough and the contribution of paracellular ion transport pathways is low, the ion transport through paracellular channels formed by tight junction proteins and the transcellular transport of ions (via transporters) is measured.[55,56] Measuring the TEER has the great advantage over the permeability measurements described before that it is a quick, non-invasive and label-free way to assess barrier tightness. In addition, if a suitable electrode material and measurement method are chosen and the measurement electrodes are integrated into a microfluidic BBB-on-chip device, the measurements can be performed in real-time.[35,55]

To be able to compare barrier resistances between different devices and Transwell platforms, the measured resistance of the endothelial barrier (R_{endo} in Ω, if needed corrected for the resistance of e.g. channels and membranes) is normalized by multiplying it with the area through which the resistance has been measured (A in cm^2), resulting in the TEER:

$$TEER = R_{endo} \cdot A [\Omega \cdot cm^2]$$

Electrically, the inverse of TEER corresponds to the conductance per unit area. Sometimes the resistance is erroneously normalized by dividing it by area, resulting in an error of factor A^2.[17,46] In a device with two perpendicular channels separated by a membrane, the area relevant for the TEER is represented by the membrane surface at the channel junction.[35,40] In such configurations, one has to take into account that microfluidic channels can have a high electrical resistance when they have small dimensions: the resistance scales inversely to the cross-sectional area of the channel. Therefore, the electrodes need to be positioned smartly and preferably be fixed in place to prevent measurement errors by differences in electrode placement.[53] Another possible issue that was pointed out by Odijk *et al.* is that the distribution of the electrical current may not be uniform across the membrane interface in microfluidic devices, resulting in an overestimation of the TEER. This can be corrected with the mathematical model presented in this publication.[53]

Measuring TEER with impedance spectroscopy (using alternating currents; AC) is preferred over measuring the ohmic resistance with DC. Using AC currents at the proper frequencies prevents electrode and concentration polarization, and other DC-related effects on the cells.[54,55] Furthermore, measuring the impedance at different AC frequencies gives more information about the cell culture and even enables direct measurement of the TEER without having to correct for the resistance of the device without cells.[52]

Next to device characteristics, for which can be compensated mathematically, also other factors will influence electrical resistance measurements. Analogously to the permeability measurements specified above, TEER measurements will be influenced by the presence of co-cultured cells. The presence of extra cells will provide an extra obstacle for ion transport, resulting in a higher resistance than what would result from the tight endothelium alone. In addition, TEER measurements are sensitive to temperature and the ionic composition of the culture medium.[37] These factors have to be kept constant in TEER measurement protocols.

In conclusion, TEER is a very valuable indicator of barrier tightness that can be measured quickly, non-invasively, label-free and real-time. However, how the TEER is measured needs to be well-thought-through to arrive at valid TEER values and to be able to compare between platforms.

Cells

The cells used are important for the physiological relevance of the BBB-on-chip. The more closely the cells mimic the human

BBB, the more predictive the model is expected to be. Until now, many of the BBB-on-chip models and other *in vitro* BBB models use cells from animal sources.[17,53] Using these cells can provide valuable information for validation purposes, because the *in vitro* results can be more easily compared to *in vivo* results from the same species. However, human cells would be the most predictive and would thus be the cells of choice for future drug development applications.

Endothelial cells derived from brain capillaries already have the appropriate expression profile, so these will be the first choice. However, retaining this phenotype *in vitro* after several passages has been challenging.[17] In addition, human brain tissue and therefore primary human brain endothelial cells are scarce.[17] Although challenging to make, brain-derived endothelial cell lines are more readily available and provide less batch-to-batch difference, but they also lost part of their phenotype (and possibly genotype) during the immortalization process.[17] In contrast, advances have been made in deriving brain-specific endothelial cells from human induced pluripotent stem cells (hiPSC).[57,58] This development holds great promise for personalized (or precision) medicine, since brain endothelium can be derived from both "healthy" cells and "diseased" cells (e.g., with genetic defects resulting in BBB pathology *in vivo*), as well as from cells originating from different people or populations.[9,59]

As was mentioned in the introduction, next to endothelial cells also other cells from the NVU, such as astrocytes and pericytes, are important for the formation and maintenance of the barrier. [2,4,60] The model will be more physiologically relevant if these cell types are included as well and some of the current BBBs-on-chips have already showed an increase in barrier tightness when these cells are included.[35,41,46] However, in most of these devices the 2 cell types are cultured in different channels or chambers, separated by a membrane with a thickness of several micrometers. A thinner membrane allowing cell-cell contact or having no membrane would be more physiological, but also more challenging to fabricate and test reproducibly. For this purpose hydrogel-based devices, such as the ones by Kim and Cho,[44,45] are expected to be beneficial, because they allow direct contact between the endothelial cells lining the lumen and the other cells that are cultured in 3D in the surrounding gel. On the other hand, these devices are more difficult to fabricate and it is more difficult to image the cells inside the device and test the permeability and TEER.

To conclude this section, animal cells are widely used and enable easy comparison of *in vitro* results to *in vivo* tests within the same species. However, the use of human cells in BBBs-on-chips would be most informative for drug development studies or studies of human BBB physiology and pathology, although the tissue source has limited availability. Recent advances show that deriving brain endothelium from human iPS cells potentially provides a more accessible source of relevant cells.

Shear stress

Exposing the endothelium to fluid flow and the associated wall shear stress is reported to have positive effects on endothelial differentiation and cell function, which is expected as such shear flow occurs in the natural environment.[61-64] Microfluidic devices are especially suited for incorporation of fluid flow and shear stress, which is difficult in conventional *in vitro* (Transwell) models, thus presenting a real operational advantage of microfluidic models. The positive effect of shear stress on BBB tightness has already been demonstrated in several BBBs-on-chips,[35,36,40] but shear stress is not yet standardly applied. Furthermore, as was already mentioned before, the wall shear stress is not always of physiological level, which is 0.3-2 Pa for brain capillaries.[37,38] For a channel with a rectangular cross-section and with a steady laminar flow of a Newtonian fluid, the shear stress is calculated as:

$$\tau = \frac{6 \cdot \mu \cdot Q}{w \cdot h^2} \cdot \left(1 + \frac{h}{w}\right) \cdot f^*\left(\frac{h}{w}\right) [\mathrm{Pa}]$$

in which τ is the shear stress (Pa), μ is the viscosity of the fluid used in the microfluidic channel (Pa·s), Q is the volumetric flow rate (m^3/s), and w and h are the channel width (surface of endothelial culture; m) and height (m), respectively.[65] The function $f^*(x)$ is an infinite summation series of which the output values for most common input values are listed in ref. 65. If the channel width is much larger than the channel height ($w >> h$) and the aspect ratio h/w approaches zero, this equation reduces to $\tau = \frac{6 \cdot \mu \cdot Q}{w \cdot h^2}$. To approximate the viscosity of culture medium the viscosity of water at 37°C can be used, which is 0.7 mPa·s.[37]

In a tube with a circular cross-section the wall shear stress will be equal along the entire inner wall because of the cylindrical symmetry. However, inside a rectangular channel the shear stress will not be uniform across the channel width because of the presence of the side walls. Therefore, to achieve a mostly uniform shear stress on all cells across the channel width, the width should be much higher than the height ($w \rangle\rangle h$), resulting in a flat flow profile. This situation is illustrated in **Figure 3** for different aspect ratios (channel height over channel width). The flow profile in a channel with a rectangular cross-section can be approximated with the following equations:

$$\frac{u_{x,y}}{u_{max}} = \left[1 - \left(\frac{2x}{h}\right)^2\right]\left[1 - \left|\frac{2y}{w}\right|^m\right]; \quad m = \frac{w}{h}\sqrt{2} + 0.89\frac{h}{w}$$

In these equations $u_{x,y}$ is the fluid velocity at a given position *(x,y)* inside the channel cross-section, which is scaled to the maximum velocity, u_{max}, h is the channel height and w is the channel width (with $w > h$).[66] The resulting flow profile for Prabhakarpandian's chip[42] with $\frac{h}{w} = \frac{100\mu m}{200\mu m} = 0.5$ is shown in **Figure 3A**, while the flow profile in Booth's chip[35] with $\frac{h}{w} = \frac{200\mu m}{2mm} = 0.1$ is shown in **Figure 3B**. The lower aspect ratio of the Booth chip results in a much more uniform flow profile across the channel width. In **Figure 3C** the flow profiles for more aspect ratios are shown, clearly demonstrating that a smaller aspect ratio *h/w* results in a more uniform flow profile. All flow profiles were modeled and displayed using MATLAB R2013a. The result of a non-uniform flow profile is that the cells near the side walls will always experience a lower shear than the cells in the middle of the chip. In addition, this lower flow rate at the edges results in longer

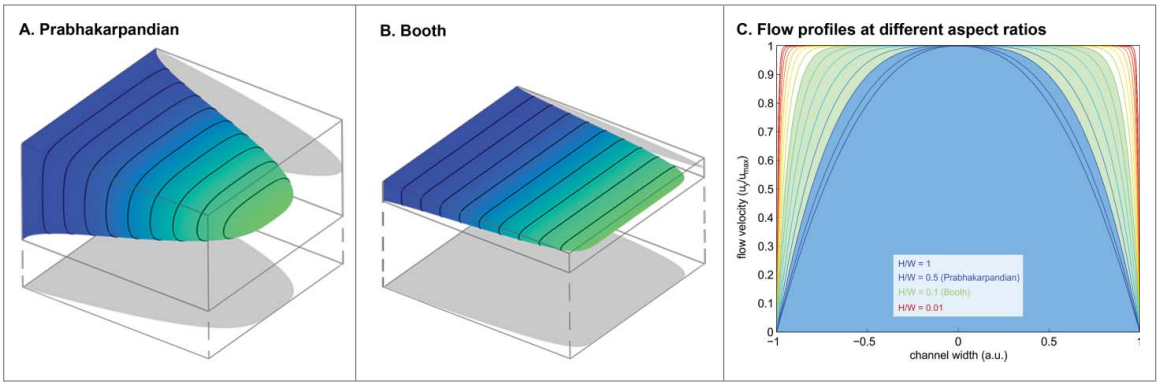

Figure 3. Flow profiles inside the BBB chip of Prabhakarpandian[42] (**A**) and Booth[35] (**B**) and at different aspect ratios (**C**), modeled with MATLAB R2013a. The endothelial cells are cultured on the bottom surface of the depicted channel.

retention times of paracrine signaling agents and analytes for permeability measurements at the edges. The mechanisms mentioned above can result in differences in cell behavior or measured permeability across the channel width. Moreover, the growth of cells in a channel can influence the flow profile and the associated shear stress. If the cells form a thick layer compared to the channel height, the average shear stress on the cells will be higher compared to the shear stress on an empty surface at the same volumetric flow rate. Epithelia are more likely to pose such problems than endothelia because of their relative thickness.

In conclusion, physiologically relevant shear stress is an important stimulus for endothelial cells. This can be applied easily on cells in a microfluidic device. However, the channel geometry influences the shear stress distribution on the cells. In a rectangular channel the most uniform shear stress is achieved if the channel height is much smaller than the channel width.

Conclusion

The use of BBBs-on-chips has great potential to further the field of BBB research. In microfluidic platforms the advantages of *in vivo* and *in vitro* models are combined: organ-on-chip technologies enable the study of organ-level function like *in vivo* models, while still being robust, reproducible and easy to analyze like *in vitro* models. There are already a number of reports of BBBs-on-chips in literature that show novel approaches and promising results. These examples already show some benefits of the use of microfluidics for BBB research applications. In addition, organ–on-chip technologies provide flexibility in the design of and control over microenvironments, as well as readout protocols. This enables the development of a wide range of BBB-on-chip models that can each answer specific research questions.

However, to accelerate the development and enable comparison and validation of the BBB-on-chip models it is beneficial to have some standardization and consensus among researchers. In this review 4 aspects are highlighted. Determining the BBB permeability is an important readout of any BBB model. To enable comparison between platforms, the barrier permeability should be reported as universal values, such as permeability coefficients. Furthermore, TEER is a quick and non-invasive measure of barrier tightness. If correctly measured and calculated, TEER values can also be compared between devices. Brain microvascular endothelial cells from animal sources are more widely available, but human cells are more informative for human BBB research. iPS cells hold promise as a more accessible source of relevant cells, also suitable for personalized medicine. Lastly, the endothelial cells inside BBBs-on-chips can be exposed to physiologically relevant shear stress. Suitable channel geometries are required to achieve mostly uniform shear stress across the cell barrier.

Next to these considerations for optimal designs and protocols for BBBs-on-chips that were highlighted in this review, there are more microenvironment parameters that will benefit from a more standardized approach. Among these are the choice of chip materials and geometries, and incorporation of biological agents in the microenvironment. To this end, it is beneficial to have multidisciplinary teams developing BBBs-on-chips in order to have both biology and engineering aspects covered.[6] In addition, widespread application of microfluidic BBBs-on-chips also requires cheap fabrication, easy operation and possibility for high-throughput and parallelized models.[67] We are confident that the rapidly emerging field of BBB-on-chip models will have a real impact on biomedical science and drug development in the near future.

Disclosure of Potential Conflicts of Interest

No potential conflicts of interest were disclosed.

Acknowledgments

We would like to thank Mathijs Bronkhorst for fruitful discussions and assistance with modeling flow profiles.

Funding

This research was funded by the SRO Biomedical Microdevices and the SRO Organs-on-chips, MIRA Institute for Biomedical Technology and Technical Medicine, University of Twente, The Netherlands.

References

1. Abbott NJ. Blood–brain barrier structure and function and the challenges for CNS drug delivery. J Inherited Metab dis 2013; 36:437-49; PMID:23609350; http://dx.doi.org/10.1007/s10545-013-9608-0
2. Serlin Y, Shelef I, Knyazer B, Friedman A. Anatomy and physiology of the blood–brain barrier. Seminars Cell Dev Biol 2015; 38:2-6; http://dx.doi.org/10.1016/j.semcdb.2015.01.002
3. Pardridge WM. The blood-brain barrier: bottleneck in brain drug development. NeuroRx 2005; 2:3-14; PMID:15717053; http://dx.doi.org/10.1602/neurorx.2.1.3
4. Abbott NJ, Rönnbäck L, Hansson E. Astrocyte–endothelial interactions at the blood–brain barrier. Nat Rev Neurosci 2006; 7:41-53; PMID:16371949; http://dx.doi.org/10.1038/nrn1824
5. Abbott NJ. Prediction of blood–brain barrier permeation in drug discovery from in vivo, in vitro and in silico models. Drug Discov Today 2004; 1:407-16; http://dx.doi.org/10.1016/j.ddtec.2004.11.014
6. Wolff A, Antfolk M, Brodin B, Tenje M. In Vitro blood-brain barrier models—an overview of established models and new microfluidic approaches. J Pharmaceutical Sci 2015; 104:2727-46; http://dx.doi.org/10.1002/jps.24329
7. Huh D, Torisawa YS, Hamilton GA, Kim HJ, Ingber DE. Microengineered physiological biomimicry: organs-on-chips. Lab chip 2012; 12:2156-64; PMID:22555377; http://dx.doi.org/10.1039/c2lc40089h
8. Perrin S. Preclinical research: Make mouse studies work. Nature 2014; 507:423-5; PMID:24678540; http://dx.doi.org/10.1038/507423a
9. Pamies D, Hartung T, Hogberg HT. Biological and medical applications of a brain-on-a-chip. Exp Biol Med 2014; 239:1096-107; http://dx.doi.org/10.1177/1535370214537738
10. Hackam DG. Translating animal research into clinical benefit. BMJ: Br Med J 2007; 334:163; http://dx.doi.org/10.1136/bmj.39104.362951.80
11. van der Worp HB, Howells DW, Sena ES, Porritt MJ, Rewell S, O'Collins V, Macleod MR. Can animal models of disease reliably inform human studies. PLoS Med 2010; 7:e1000245; PMID:20361020; http://dx.doi.org/10.1371/journal.pmed.1000245
12. Shanks N, Greek R, Greek J. Are animal models predictive for humans? Philosophy Ethics Humanities Med 2009; 4:2; http://dx.doi.org/10.1186/1747-5341-4-2
13. Perrin S. Preclinical research: Make mouse studies work. Nature 2014; 507:423-5; http://dx.doi.org/10.1038/507423a
14. Shawahna R, Declèves X, Scherrmann J-M. Hurdles with using in vitro models to predict human blood-brain barrier drug permeability: a special focus on transporters and metabolizing enzymes. Curr Drug Metab 2013; 14:120-36; PMID:23215812; http://dx.doi.org/10.2174/138920013804545232
15. Naik P, Cucullo L. In vitro blood–brain barrier models: Current and perspective technologies. J Pharmaceutical Sci 2012; 101:1337-54; http://dx.doi.org/10.1002/jps.23022
16. van der Meer AD, van den Berg A. Organs-on-chips: breaking the in vitro impasse. Integrative Biol 2012; 4:461-70; http://dx.doi.org/10.1039/c2ib00176d
17. Abbott NJ, Dolman DM, Yusof S, Reichel A. In Vitro Models of CNS Barriers. In: Hammarlund-Udenaes M, de Lange ECM, Thorne RG, eds. Drug Delivery to the Brain: Springer New York, 2014:163-97
18. Hatherell K, Couraud PO, Romero IA, Weksler B, Pilkington GJ. Development of a three-dimensional, all-human< i> in vitro model of the blood–brain barrier using mono-, co-, and tri-cultivation Transwell models. J Neurosci Methods 2011; 199:223-9; PMID:21609734; http://dx.doi.org/10.1016/j.jneumeth.2011.05.012
19. Bhatia SN, Ingber DE. Microfluidic organs-on-chips. Nat Biotechnol 2014; 32:760-72; PMID:25093883; http://dx.doi.org/10.1038/nbt.2989
20. Moraes C, Mehta G, Lesher-Perez S, Takayama S. Organs-on-a-Chip: A Focus on Compartmentalized Microdevices. Annals Biomed Engineering 2012; 40:1211-27; http://dx.doi.org/10.1007/s10439-011-0455-6
21. Huh D, Matthews BD, Mammoto A, Montoya-Zavala M, Hsin HY, Ingber DE. Reconstituting organ-level lung functions on a chip. Science 2010; 328:1662-8; PMID:20576885; http://dx.doi.org/10.1126/science.1188302
22. Kim HJ, Huh D, Hamilton G, Ingber DE. Human gut-on-a-chip inhabited by microbial flora that experiences intestinal peristalsis-like motions and flow. Lab Chip 2012; 12:2165-74; PMID:22434367; http://dx.doi.org/10.1039/c2lc40074j
23. Kim HJ, Ingber DE. Gut-on-a-Chip microenvironment induces human intestinal cells to undergo villus differentiation. Integrative Biol 2013; 5:1130-40; PMID:23817533; http://dx.doi.org/10.1039/c3ib40126j
24. Westein E, van der Meer AD, Kuijpers MJE, Frimat JP, van den Berg A, Heemskerk JWM. Atherosclerotic geometries exacerbate pathological thrombus formation poststenosis in a von Willebrand factor-dependent manner. Proc Natl Acad Sci 2013; 110:1357-62; PMID:23288905; http://dx.doi.org/10.1073/pnas.1209905110
25. Nedergaard M. Garbage Truck of the Brain. Science (New York, NY) 2013; 340:1529-30; http://dx.doi.org/10.1126/science.1240514
26. Iliff JJ, Nedergaard M. Is there a cerebral lymphatic system? Stroke; J Cerebral Circulation 2013; 44:S93-S5; http://dx.doi.org/10.1161/STROKEAHA.112.678698
27. van der Meer AD, Wolbers F, Vermes I, van den Berg A. Blood-brain Barrier (BBB): An Overview of the Research of the Blood-brain Barrier Using Microfluidic Devices. In: van den Berg A, Segerink LI, eds. Microfluidics for Med Applications, 2014:40-56
28. Adriani G, Ma D, Pavesi A, Goh E, Kamm RD. A microfluidic model of the blood brain barrier. 4th THERMIS World Congress. Boston, USA: Tissue Engineering Part A, 2015:S40-S
29. Yeste J, Illa X, Guimerà A, Villa R. A novel strategy to monitor microfluidic in-vitro blood-brain barrier models using impedance spectroscopy. Bio-MEMS and Medical Microdevices II. Barcelona, Spain: SPIE Conference Proceedings, 2015:95180N-N-6
30. van der Helm MW, Odijk M, Frimat J-P, Eijkel JC, van den Berg A, Segerink LI. Simple and stable transendothelial electrical resistance measurements in organs-on-chips. The 19th International Conference on Miniaturized Systems for Chemistry and Life Sciences. Gyeongju, South Korea, 2015
31. Xu H, Li ZY, Yu Y, Qin JH. Microfluidic high-throughput 3D blood-brain barrier model in vitro for drug testing in brain tumor. The 19th International Conference on Miniaturized Systems for Chemistry and Life Sciences. Gyeongju, South Korea, 2015
32. Xu H, Zhang M, Wang L, Qin JH. Organ-on-a-chip for drug testing in brain diseases. The 19th International Conference on Miniaturized Systems for Chemistry and Life Sciences. Gyeongju, South Korea, 2015
33. Benson BL, Cotleur AC, Shimizu F, Takeshita Y, Winger RC, Huang A, Marsh G, Ligresti G, Muller WA, Kanda T, et al. Leukocyte-endothelial interactions at the blood-brain barrier studied in fully-human flow-based in vitro models incorporating microfluidics. 14th Annual World Preclinical Congress. Boston, USA, 2015
34. van der Meer AD, Ingber DE, Herland A. Blood brain barrier-on-chip. 14th Annual World Preclinical Congress, Boston, USA, 2015
35. Booth R, Kim H. Characterization of a microfluidic in vitro model of the blood-brain barrier (mu BBB). Lab Chip 2012; 12:1784-92; PMID:22422217; http://dx.doi.org/10.1039/c2lc40094d
36. Booth R, Kim H. Permeability Analysis of Neuroactive Drugs Through a Dynamic Microfluidic In Vitro Blood-Brain Barrier Model. Annals Biomed Engineering 2014; 42:2379-91; http://dx.doi.org/10.1007/s10439-014-1086-5
37. Wong AD, Ye M, Levy AF, Rothstein JD, Bergles DE, Searson PC. The blood-brain barrier: an engineering perspective. Frontiers Neuroengineering 2013; 6:7; http://dx.doi.org/10.3389/fneng.2013.00007
38. Desai SY, Marroni M, Cucullo L, Krizanac-Bengez L, Mayberg MR, Hossain MT, Grant GG, Janigro D. Mechanisms of endothelial survival under shear stress. Endothelium 2002; 9:89-102; PMID:12200960; http://dx.doi.org/10.1080/10623320212004
39. Yeon JH, Na D, Choi K, Ryu SW, Choi C, Park JK. Reliable permeability assay system in a microfluidic device mimicking cerebral vasculatures. Biomed Microdevices 2012; 14:1141-8; PMID:22821236; http://dx.doi.org/10.1007/s10544-012-9680-5
40. Griep LM, Wolbers F, de Wagenaar B, ter Braak PM, Weksler BB, Romero IA, Couraud PO, Vermes I, van der Meer AD, van den Berg A. BBB ON CHIP: microfluidic platform to mechanically and biochemically modulate blood-brain barrier function. Biomed Microdevices 2013; 15:145-50; PMID:22955726; http://dx.doi.org/10.1007/s10544-012-9699-7
41. Achyuta AKH, Conway AJ, Crouse RB, Bannister EC, Lee RN, Katnik CP, Behensky AA, Cuevas J, Sundaram SS. A modular approach to create a neurovascular unit-on-a-chip. Lab Chip 2013; 13:542-53; PMID:23108480; http://dx.doi.org/10.1039/C2LC41033H
42. Prabhakarpandian B, Shen MC, Nichols JB, Mills IR, Sidoryk-Wegrzynowicz M, Aschner M, Pant K. SyM-BBB: a microfluidic blood brain barrier model. Lab Chip 2013; 13:1093-101; PMID:23344641; http://dx.doi.org/10.1039/c2lc41208j
43. Deosarkar SP, Prabhakarpandian B, Wang B, Sheffield JB, Krynska B, Kiani MF. A Novel Dynamic Neonatal Blood-Brain Barrier on a Chip. PLoS One 2015; 10: e0142725; PMID:26555149; http://dx.doi.org/10.1371/journal.pone.0142725
44. Cho H, Seo JH, Wong KH, Terasaki Y, Park J, Bong K, Arai K, Lo EH, Irimia D. Three-Dimensional Blood-Brain Barrier Model for in vitro Studies of neurovascular pathology. Sci Rep 2015; 5:15222
45. Kim JA, Kim HN, Im S-K, Chung S, Kang JY, Choi N. Collagen-based brain microvasculature model in vitro using three-dimensional printed template. Biomicrofluidics 2015; 9:024115; PMID:25945141http://dx.doi.org/10.1063/1.4917508
46. Brown JA, Pensabene V, Markov DA, Allwardt V, Neely MD, Shi M, Britt CM, Hoilett OS, Yang Q, Brewer BM, et al. Recreating blood-brain barrier physiology and structure on chip: A novel neurovascular microfluidic bioreactor. Biomicrofluidics 2015; 9:054124; PMID:26576206; http://dx.doi.org/10.1063/1.4934713
47. Sellgren KL, Hawkins BT, Grego S. An optically transparent membrane supports shear stress studies in a three-dimensional microfluidic neurovascular unit model. Biomicrofluidics 2015; 9:061102; PMID:26594261; http://dx.doi.org/10.1063/1.4935594
48. Walter FR, Valkai S, Kincses A, Petneházi A, Czeller T, Veszelka S, Ormos P, Deli MA, Dér A. A versatile lab-on-a-chip tool for modeling biological barriers. Sensors Actuators B: Chem 2016; 222:1209-19; http://dx.doi.org/10.1016/j.snb.2015.07.110
49. Chaitanya GV, Cromer WE, Wells SR, Jennings MH, Couraud PO, Romero IA, Weksler B, Erdreich-Epstein A, Mathis JM, Minagar A. Gliovascular and cytokine interactions modulate brain endothelial barrier in vitro. J Neuroinflammation 2011; 8:162; PMID:22112345; http://dx.doi.org/10.1186/1742-2094-8-162

50. Yuan F, Leunig M, Berk DA, Jain RK. Microvascular permeability of albumin, vascular surface area, and vascular volume measured in human adenocarcinoma LS174T using dorsal chamber in SCID mice. Microvascular Res 1993; 45:269-89; http://dx.doi.org/10.1006/mvre.1993.1024
51. Li G, Simon MJ, Cancel LM, Shi ZD, Ji X, Tarbell JM, Morrison B, III, Fu BM. Permeability of endothelial and astrocyte cocultures: in vitro blood–brain barrier models for drug delivery studies. Annals Biomed Engineering 2010; 38:2499-511; http://dx.doi.org/10.1007/s10439-010-0023-5
52. Srinivasan B, Kolli AR, Esch MB, Abaci HE, Shuler ML, Hickman JJ. TEER Measurement Techniques for In Vitro Barrier Model Systems. Jala 2015; 20:107-26; PMID:25586998
53. Odijk M, van der Meer AD, Levner D, Kim HJ, van der Helm MW, Segerink LI, Frimat J-P, Hamilton GA, Ingber DE, van den Berg A. Measuring direct current trans-epithelial electrical resistance in organ-on-a-chip microsystems. Lab Chip 2015; 15:745-52; PMID:25427650; http://dx.doi.org/10.1039/C4LC01219D
54. Thuenauer R, Rodriguez-Boulan E, Romer W. Microfluidic approaches for epithelial cell layer culture and characterisation. Analyst 2014; 139:3206-18; PMID:24668405; http://dx.doi.org/10.1039/C4AN00056K
55. Benson K, Cramer S, Galla HJ. Impedance-based cell monitoring: barrier properties and beyond. Fluids Barriers CNS 2013; 10:5; PMID:23305242; http://dx.doi.org/10.1186/2045-8118-10-5
56. Krug SM, Fromm M, Günzel D. Two-Path impedance spectroscopy for measuring paracellular and transcellular epithelial resistance. Biophysical J 2009; 97:2202-11; http://dx.doi.org/10.1016/j.bpj.2009.08.003
57. Lippmann ES, Al-Ahmad A, Azarin SM, Palecek SP, Shusta EV. A retinoic acid-enhanced, multicellular human blood-brain barrier model derived from stem cell sources. Scientific Rep 2014; 4:4160
58. Lippmann ES, Azarin SM, Kay JE, Nessler RA, Wilson HK, Al-Ahmad A, Palecek SP, Shusta EV. Derivation of blood-brain barrier endothelial cells from human pluripotent stem cells. Nat Biotechnol 2012; 30:783-91; PMID:22729031; http://dx.doi.org/10.1038/nbt.2247
59. Bellin M, Marchetto MC, Gage FH, Mummery CL. Induced pluripotent stem cells: the new patient? Nat Rev Mol Cell Biol 2012; 13:713-26; PMID:23034453; http://dx.doi.org/10.1038/nrm3448
60. He YR, Yao Y, Tsirka SE, Cao Y. Cell-Culture Models of the Blood-Brain Barrier. Stroke 2014; 45:2514-26; PMID:24938839; http://dx.doi.org/10.1161/STROKEAHA.114.005427
61. Van der Meer A, Poot A, Feijen J, Vermes I. Analyzing shear stress-induced alignment of actin filaments in endothelial cells with a microfluidic assay. Biomicrofluidics 2010; 4:011103; http://dx.doi.org/10.1063/1.3366720
62. Booth R, Noh S, Kim H. A multiple-channel, multiple-assay platform for characterization of full-range shear stress effects on vascular endothelial cells. Lab Chip 2014; 14:1880-90; PMID:24718713; http://dx.doi.org/10.1039/c3lc51304a
63. Gulino-Debrac D. Mechanotransduction at the basis of endothelial barrier function. Tissue Barriers 2013; 1: e24180; PMID:24665386; http://dx.doi.org/10.4161/tisb.24180
64. Shemesh J, Jalilian I, Shi A, Heng Yeoh G, Knothe Tate ML, Ebrahimi Warkiani M. Flow-induced stress on adherent cells in microfluidic devices. Lab Chip 2015; 15:4114-27; PMID:26334370; http://dx.doi.org/10.1039/C5LC00633C
65. Son Y. Determination of shear viscosity and shear rate from pressure drop and flow rate relationship in a rectangular channel. Polymer 2007; 48:632-7; http://dx.doi.org/10.1016/j.polymer.2006.11.048
66. Vanapalli S, Van den Ende D, Duits M, Mugele F. Scaling of interface displacement in a microfluidic comparator. Appl Phys Lett 2007; 90:114109; http://dx.doi.org/10.1063/1.2713800
67. Hovell CM, Sei YJ, Kim Y. Microengineered Vascular Systems for Drug Development. J Lab Automation 2014:2211068214560767
68. Reproduced from Booth R, Kim H. Characterization of a microfluidic in vitro model of the blood-brain barrier (mu BBB). Lab Chip 2012; 12:1784-92, with permission of The Royal Society of Chemistry; PMID:22422217; http://dx.doi.org/10.1039/c2lc40094d
69. Yeon JH, Na D, Choi K, Ryu SW, Choi C, Park JK. With kind permission from Springer Science+Business Media: Biomedical Microdevices, Reliable permeability assay system in a microfluidic device mimicking cerebral vasculatures 2012; 14:1141-1148, figure 1b; PMID:22821236
70. Griep LM, Wolbers F, de Wagenaar B, ter Braak PM, Weksler BB, Romero IA, Couraud PO, Vermes I, van der Meer AD, van den Berg A. With kind permission from Springer Science+Business Media: Biomedical Microdevices, BBB ON CHIP: microfluidic platform to mechanically and biochemically modulate blood-brain barrier function 2013; 15:145-150, figure 1a and 1c; PMID:22955726
71. Reproduced from Achyuta AKH, Conway AJ, Crouse RB, Bannister EC, Lee RN, Katnik CP, Behensky AA, Cuevas J, Sundaram SS. A modular approach to create a neurovascular unit-on-a-chip. Lab Chip 2013; 13:542-53, with permission of The Royal Society of Chemistry; PMID:23108480; http://dx.doi.org/10.1039/C2LC41033H
72. Reproduced fromPrabhakarpandian B, Shen MC, Nichols JB, Mills IR, Sidoryk-Wegrzynowicz M, Aschner M, Pant K. SyM-BBB: a microfluidic blood brain barrier model. Lab Chip 2013; 13:1093-101, with permission of The Royal Society of Chemistry; PMID:23344641; http://dx.doi.org/10.1039/c2lc41208j
73. Reproduced with permission from Kim JA, Kim HN, Im SK, Chung S, Kang JY, Choi N. Collagen-based brain microvasculature model in vitro using three-dimensional printed template. Biomicrofluidics 2015; 9:024115. Copyright 2015, AIP Publishing LLC
74. Reprinted with permission from Brown JA, Pensabene V, Markov DA, Allwardt V, Neely MD, Shi M, Britt CM, Hoilett OS, Yang Q, Brewer BM, et al. Recreating blood-brain barrier physiology and structure on chip: A novel neurovascular microfluidic bioreactor. Biomicrofluidics 2015; 9:054124. Copyright 2015, AIP Publishing LLC
75. Reprinted with permission from Sellgren KL, Hawkins BT, Grego S. An optically transparent membrane supports shear stress studies in a three-dimensional microfluidic neurovascular unit model. Biomicrofluidics 2015; 9:061102. Copyright 2015, AIP Publishing LLC
76. Reprinted from Sensors and Actuators B: Chemical, 222, Walter FR, Valkai S, Kincses A, Petneházi A, Czeller T, Veszelka S, Ormos P, Deli MA, Dér A. A versatile lab-on-a-chip tool for modeling biological barriers, 1209-1219, Copyright 2016, with permission from Elsevier